

Potential energy curves of the 5s Rydberg excited states and ionized states of Kr₂ studied by the SAC–CI theory¹

Yoshihiro Mizukami

*Division of Molecular Engineering, Graduate School of Engineering, Kyoto University,
Kyoto 606 (Japan)*

Hiroshi Nakatsuji

*Department of Synthetic Chemistry, Faculty of Engineering, Kyoto University, Kyoto 606
(Japan)*

(Received 30 August 1990)

Abstract

Potential energy curves of the 5s Rydberg excited states and ionized states of Kr₂ are studied by symmetry adapted cluster–configuration interaction (SAC–CI) theory. New assignments for the observed peaks of the near infrared absorptions from the lowest excited state are proposed. Calculated transition energies from the ground state to the lowest excited states are comparable with those from the laser absorption experiment. The experimental vertical and adiabatic ionization potential are well reproduced from the potential curves of the ionized states.

INTRODUCTION

The recent development of VUV-laser induced fluorescence spectroscopy makes it possible to reveal the nature of the excited states of rare-gas dimers [1–3]. Theoretical studies on the other hand, have provided useful information on the global nature of the potential energy curves. We have calculated the potential energy curves of the ground, excited and ionized states of Ar₂ by the symmetry adapted cluster–configuration interaction (SAC–CI) theory [4]. Our theoretical potential curves have provided the transition energies for both of the absorptions and emissions in good agreement with the experimental values. We have also studied the absorption spectra from the excited state of Ar₂ and provided a new assignment. These results assure that the SAC/SAC–CI method is useful for calculating potential energy curves of the ground and excited states of van der Waals systems. Dunning and Hay have calculated the excited state potential curves for the open-shell van der Waals molecules ArF,

¹Dedicated to Professor George G. Hall for his activity at Kyoto University.

KrF and XeF [5]. These theoretical curves are useful for studying the mechanisms of laser emission processes.

We study in this paper the potential energy curves of the excited and ionized states of Kr_2 by the SAC/SAC-CI method. The excited states of the Kr dimer are well known as a laser emission source. Despite its importance, there are only a few theoretical studies on the excited states of Kr_2 , mainly by Gadea and Spiegelmann (GS) [6,7] who have performed CI calculations using pseudopotentials and have obtained the potential curves of some lower excited states. However, there is no theoretical work which focuses on the spectroscopic properties, particularly the near infrared absorptions from the lowest bound excited states of Kr_2 observed by Arai et al. [8]. Here, we report the potential energy curves of the 5s Rydberg excited states of Kr_2 . We give an assignment for the upper states of the absorption spectra observed by Arai et al. LaRocque et al. observed fluorescence excitation spectra of three band systems of Kr_2 [2] and have reported very accurate transition energies from the potential minimum of the ground state to the upper 5s Rydberg states A(1_u), B(O_u^+) and C(O_u^+). We compare our theoretical results with these experimental data.

We also report the potential curves of the ionized states of Kr_2 . In our previous work on Ar_2 [4], we have shown that the SAC-CI method is very useful for calculating ionized states of weakly interacting systems. We compare the calculated ionization potentials of Kr_2 with the photoionization experiments.

METHOD OF CALCULATION

The ground state Hartree-Fock wave function of Kr_2 was calculated by the program GAMESS [9]. The basis set is shown in Table 1. These bases are taken from Huzinaga's table [10] and the s and p functions for outer shells are split double- ζ and triple- ζ functions, respectively. Two d functions are added as polarization functions. We use four Rydberg s and two Rydberg p functions following Spiegelmann and Gadea [7].

The correlated wave functions for the ground and excited states were calculated by the SAC/SAC-CI method. The details of the SAC/SAC-CI theory have been reported elsewhere [11,12]. Many applications are also shown in ref. 13. We used the program package SAC85 [14]. The threshold for the perturbation selections in the SAC/SAC-CI calculations are $\lambda_g = 1.0 \times 10^{-5}$ and $\lambda_e = 1.0 \times 10^{-5}$ hartree [15]. All configurations which have coefficients larger than 0.0835 in the SE-CI are used as main reference configurations [15].

POTENTIAL CURVES OF 5s RYDBERG STATES OF Kr_2

The total energies of the ground state of Kr_2 are listed in Table 2. The van der Waals minimum should appear near 7.591 bohr, but is not reproduced in the present calculation. Since the van der Waals energy is very small, its cal-

TABLE 1

Basis set of Kr used in the present calculations

Shell	Exponent	Coefficient		
Outer	s	18990.321	0.0170036	
		2863.2884	0.1193618	
		649.58505	0.4365613	
		175.03786	0.5593600	
	s	262.24460	-0.1106834	
		29.573679	0.6464273	
		12.459722	0.4260356	
	s	22.925626	-0.2414622	
		3.8683898	0.7529089	
		1.6809618	0.3833081	
		s	2.6079105	-0.2392303
		0.44479912	0.7301479	
	s	0.16799905	1.0	
Outer	p	820.11422	0.0268826	
		192.54933	0.1765619	
		59.813230	0.5628124	
		20.451806	0.4615069	
	p	9.3219035	0.3311094	
		3.7297257	0.5038281	
		1.5422929	0.2068282	
		p	0.72202413	1.0
		p	0.27801808	1.0
		p	0.10446752	1.0
	Rydberg	d	68.889745	0.0559334
			19.235851	0.2738328
		6.2805882	0.5328788	
		1.9877968	0.4009652	
s		0.035839	1.0	
s		0.0287413	1.0	
s		0.01134525	1.0	
s		0.006	1.48	
		0.002	0.08	

TABLE 1 (continued)

Shell	Exponent	Coefficient	
	p	0.035839	0.375
		0.015127	0.656
		0.0448	0.092
	p	0.0048	0.8782
		0.002	0.2142
Polarization	d	0.53	1.0
	d	0.14	1.0

TABLE 2

Calculated total energies of the ground state, $X(^1\Sigma_g^+)$ of Kr_2 at various nuclear separations

R (bohr)	Energy ^a (hartree)
4.5	-0.39728
5.0	-0.46399
5.1	-0.47264
5.2	-0.47967
5.3	-0.48565
5.6	-0.49893
6.0	-0.50859
7.0	-0.51614
8.0	-0.51682
10.0	-0.51794

^aThe energy reference is -5499 hartree.

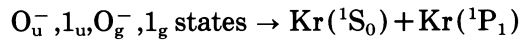
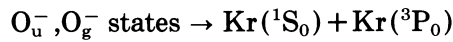
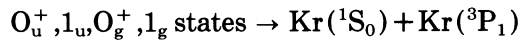
ulation would be difficult as we use approximations such as configuration selection, etc.

The potential energy curves of the singlet and triplet 5s Rydberg excited states of Kr_2 are shown in Fig. 1. They do not include spin-orbit coupling. As predicted by Mulliken for rare-gas dimers [16], the singlet and triplet Σ_u^+ states have deep minima. In our curve, this minimum is at 5.5 bohr. The ${}^3\Pi_g$ state has a shallow minimum at 5.2 bohr because of the avoided crossing between the 5s and 5p Rydberg states. The Π_u and Σ_g^+ states are repulsive throughout, though the Σ_g^+ state has a shoulder at about 6.5 bohr.

The spin-orbit (S-O) interactions are included by the atoms-in-molecule method of Cohen and Schneider [17]. This method is shown to be very useful in studies of the excited states of Ne_2 [18] and Ar_2 [4]. The S-O coupling constant is $\zeta_{4p} = 0.0158557$ hartree, which is taken from the energy level spacing of the 5s Rydberg states of the Kr atom.

$$\zeta_{4p} = (2/3) [E(^3P_2) - E(^3P_0)] \quad (1)$$

The potential curves including the S-O coupling are shown in Fig. 2 for the ungerade states and in Fig. 3 for the gerade states. Four singlet and four triplet states are mixed and split into 16 states after including the S-O coupling. At large nuclear separations, these states dissociate into the following four states as:



In Table 3 we compare the energy levels of Kr_2 at $R = 12$ bohr with the atomic spectra [19]. The theoretical values agree with the experimental value to within 0.09 eV. The vibrational frequencies ω_e , anharmonicity constant $\omega_e x_e$ and dissociation energy D_0 are calculated by fitting to the extended Morse curve [20] and are summarized in Table 4. Killeen and Eden [21] observed the excitation spectra of $^3\Pi_g(np) \leftarrow ^3\Sigma_u(5p)$ ($n=6-16$) for the electron beam excited Kr excimer. From the vibrational analysis, they determined the values of ω_e and D_0

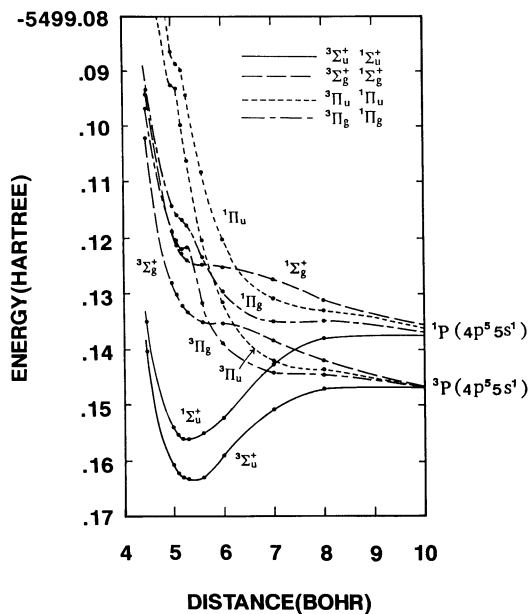


Fig. 1. Potential energy curves of the singlet and triplet 5s Rydberg excited states of Kr_2 calculated without including spin-orbit interactions.

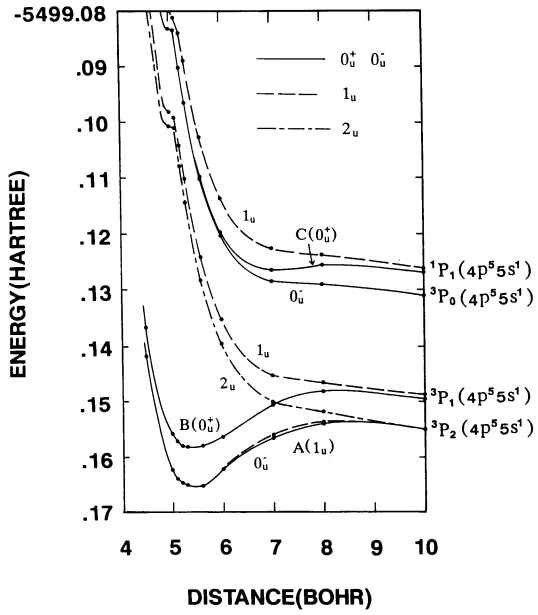


Fig. 2. Potential energy curves of the 5s Rydberg excited ungerade states of Kr_2 calculated including spin-orbit interaction.

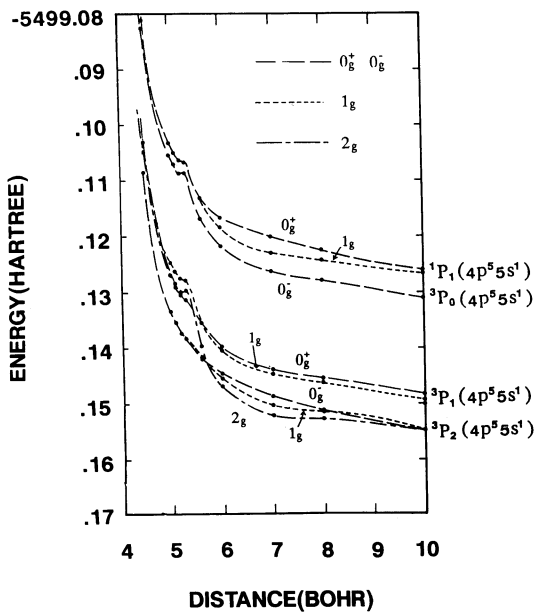


Fig. 3. Potential energy curves of the 5s Rydberg excited gerade states of Kr_2 calculated including spin-orbit interactions.

TABLE 3

The energy levels of the 5s Rydberg excited states of Kr₂ calculated at $R = 12$ bohr compared with the Kr atom spectra

State	Kr ₂ ($R = 12$ bohr) calcd. (eV)	Kr atom exptl. ^a (eV)
³ P ₂	9.873	9.915
³ P ₁	10.024	10.033
³ P ₀	10.522	10.563
¹ P ₁	10.636	10.644

^aRef. 19.

TABLE 4

Calculated spectroscopic constants of the 5s Rydberg excited states of Kr₂
Experimental values are given in parentheses

State	R_{\min} (bohr)	ω_e (cm ⁻¹)	$\omega_e x_e$ (cm ⁻¹)	D_0 (eV)
<i>Without S-O coupling</i>				
¹ Σ_u^+	5.29	121.4	0.0179	0.490
¹ Π_g	7.29	32.5	2.64	0.0043
³ Σ_u^+	5.44	147.9	1.14	0.439
<i>Including S-O coupling</i>				
Al _u (³ P ₂)	5.49	135.3 (172.0) ^a	1.26	0.314 (0.48) ^a
BO _u ⁺ (³ P ₁)	5.37	102.6	0.30	0.266
CO _u ⁺ (¹ P ₁)	7.11 (6.998) ^b	57.2 (43.8) ^b	1.77 (1.18) ^b	0.020 (0.0577) ^b

^aRef. 21.

^bRef. 2.

for the A(1_u) state. Our results are smaller than the experimental values. For the C(O_u⁺) state, the present results for ω_e and $\omega_e x_e$ are comparable with those obtained from the fluorescence excitation spectra [2], but our D_0 value is smaller than the experimental value.

ABSORPTION FROM THE EXCITED STATE

Near-infrared absorption spectra from Kr excimer were observed by Arai et al. [8]. They obtained two band systems. The first has shorter wavelengths

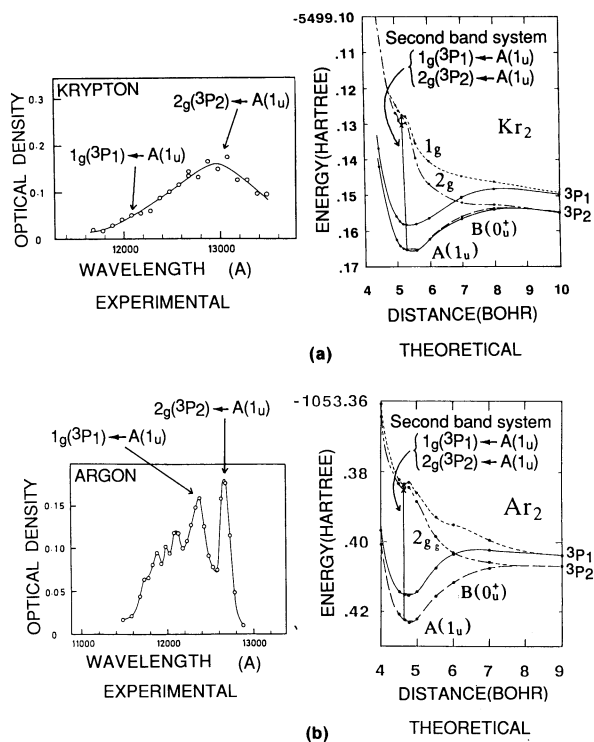


Fig. 4. Experimental spectra and theoretical potential curves for the second band systems of the near infrared absorptions of the rare-gas excimers. (a) Kr_2 (b) Ar_2 . Experimental spectra are due to Arai et al. [8].

and was assigned as the transition from the 5s to 5p Rydberg states of Kr_2 . The second was assumed to be due to the transitions within the 5s Rydberg states. Here we discuss the second band system. The observed peak is broad and asymmetric as shown in Fig. 4(a) and is assumed to be due to the transitions from the $A(1_u)$ state to the higher 5s Rydberg states. The transition energy at maximum intensity is 0.9537 eV (13 000 Å) and a shoulder seems to exist at 1.025 eV (12 100 Å).

We have calculated the transition energies from the $A(1_u)$ state to the upper states. There are three states whose transition energies are close to the experimental second band system. They are the $2_g(3P_2)$, $1_g(3P_1)$ and $O_g^+(3P_1)$ state. The $O_g^+(3P_1)$ state originates from the $1\Sigma_g^+$ state so that the transition is forbidden due to the spin symmetry. Both $2_g(3P_2)$ and $1_g(3P_1)$ states originate from the $3\Pi_g$ state so that the transitions are dipole-allowed. On the right-hand side of Fig. 4(a), we show the theoretical potential curves involved for the absorptions from the $A(1_u)$ state. We see that the $2_g(3P_2)$ state has a very shallow minimum at 5.2 bohr and the $1_g(3P_1)$ state has a shoulder. The calculated transition energies from the zero point vibrational level of the $A(1_u)$

TABLE 5

Transition energies of Kr_2 from the $A(1_u)$ state to the upper states

Initial state	Final state	Transition energy (eV)	
		Expt l. ^a	Calcd.
$A(1_u) v=0$	$2_g(^3P_2)$	0.9537	0.9564
$A(1_u) v=0$	$1_g(^3P_1)$	1.025	1.023

^aRef. 8.

state to the minimum of the $2_g(^2P_2)$ state at 5.2 bohr is 0.9564 eV, and to the shoulder of the $1_g(^3P_1)$ state at 5.2 bohr is 1.023 eV. These values are comparable with the experimental transition energies of 0.9537 eV at the maximum intensity and 1.025 eV at the shoulder. We then assign the $2_g(^3P_2)$ state to the main upper state of the spectra and the $1_g(^3P_1)$ state to the shoulder of the spectra. Table 5 is a summary of the results.

In our previous work for Ar_2 [4], we discussed the transitions from the lowest to the upper excited states. Figure 4(b) shows our theoretical potential curves of Ar_2 and the experimental peaks of Arai et al. [8]. The observed spectra show two notable peaks and theoretically we obtain shallow minima for both the $2_g(^3P_2)$ and $1_g(^3P_1)$ states. We have assigned the transitions, $1_g(^3P_1) \leftarrow A(1_u)$ and $2_g(^3P_2) \leftarrow A(1_u)$ to the lower and higher peaks, respectively [4].

COMPARISON WITH THE ABSORPTION SPECTRA

The VUV-absorption spectra of Kr_2 were first reported by Tanaka et al. [22]. They observed eight band systems and the three lowest were assigned as the absorptions from the ground state to the 5s Rydberg excited states $A(1_u)$, $B(O_u^+)$ and $C(O_u^+)$. Recently, LaRocque et al. [2] observed the rovibronic spectra for the three lowest excited states of Kr_2 by their VUV-laser fluorescence excitation spectroscopy. They obtained very reliable spectroscopic constants for both the ground $X(O_g^+)$ and third $C(O_u^+)$ states. They also obtained absorption spectra for the highest vibrational levels of the $A(1_u)$ and $B(O_u^+)$ states. We compare our calculated transition energies for the excitations, $A(1_u)$, $B(O_u^+)$, $C(O_u^+) \leftarrow X(O_g^+)$ with their results. Since we failed to obtain the potential minimum for the ground state curve, the energy at the experimental minimum ($R=7.591$ u) is taken as the lower state reference energy. The resulting transition energies are summarized in Table 6. The theory agrees with experiment to within 0.1 eV.

TABLE 6

Transition energies between the ground state $X(O_g^+)$ and the 5s Rydberg excited states $A(1_u)$, $B(O_u^+)$ and $C(O_u^+)$

Initial state	Final state	Transition energy (eV)	
		Calcd.	Expt l.
<i>Absorption</i>			
$X(O_g^+)$	$A(1_u)$	9.866 ^a	9.856 ~ 9.900 ^b
$X(O_g^+)$	$B(O_u^+)$	10.021 ^a	9.923 ~ 9.988 ^b
$X(O_g^+)$	$C(O_u^+)$	10.626 ^a	10.60 ^{b,c}

^aRelative to the ground state energy at $R_{\min}(\text{exptl.}) = 7.591$ bohr.

^bRef. 2.

^cVibrational level of the upper state $C(O_u^+)$ is $v' = 0$.

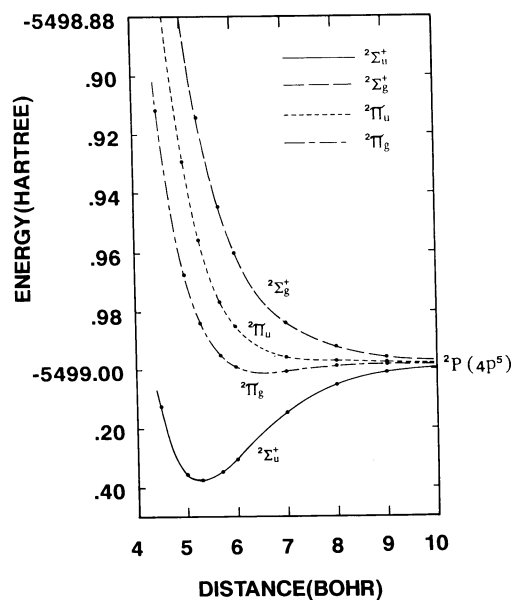


Fig. 5. Potential energy curves of the ionized states of Kr_2 calculated without including spin-orbit interactions.

POTENTIAL CURVES OF THE IONIZED STATE OF Kr_2

Rare-gas ions are important species which show laser emissions in the VUV region. Recently, the dynamics of rare-gas ion clusters have been extensively

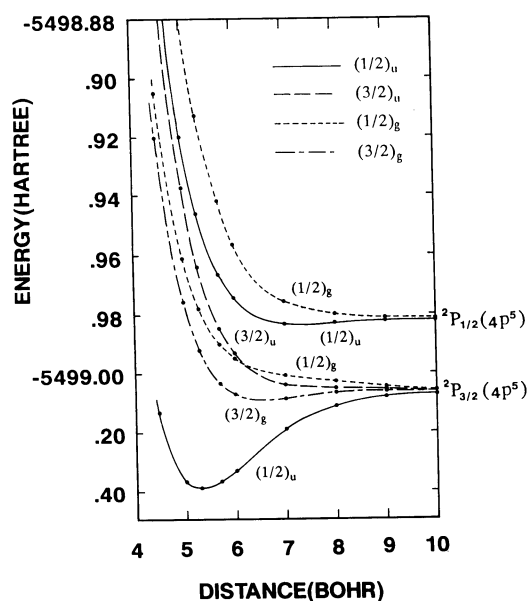


Fig. 6. Potential energy curves of the ionized states of Kr_2 calculated including spin-orbit interactions.

TABLE 7

Spectroscopic constants for the ionized states of Kr_2
Experimental results are shown in parentheses

State	R_{\min} (bohr)	IP (eV)		ω_e (cm^{-1})	$\omega_e \chi_e$ (cm^{-1})	D_e (eV)
		Vertical	Adiabatic			
I(1/2) _u (² P _{3/2})	5.29	13.69 (13.76) ^a	13.01 (12.97) ^b	163.3	0.669	0.892 (1.03) ^b
I(3/2) _g (² P _{3/2})	6.57	13.86 (13.90) ^a	13.81 (13.85) ^a	58.25	1.10	0.109 (0.16) ^a
I(3/2) _u (² P _{3/2})		13.93				
I(1/2) _g (² P _{3/2})		14.01				
II(1/2) _u (² P _{1/2})	7.27	14.52 (14.57) ^a	14.51 (14.54) ^a	42.16	0.835	0.066 (0.14) ^a
II(1/2) _g (² P _{1/2})		14.64				

^aRef. 23.

^bRef. 24.

studied. Reliable potential curves are of crucial importance for these studies. Here we report the theoretical potential energy curves of Kr_2^+ calculated by the SAC-CI method.

The potential curves of Kr_2^+ calculated without including the S–O coupling are shown in Fig. 5. The $^2\Sigma_u^+$ and $^2\Pi_g$ states are made of the ionizations from the anti-bonding molecular orbitals, $4p\sigma_u$ and $4p\pi_g$ of Kr_2 , respectively, so that they become stable and have bound wells. On the other hand, ionizations from the bonding orbitals, π_u and σ_g , lead to the $^2\Pi_u$ and $^2\Sigma_g^+$ states, respectively, and their potential curves are repulsive throughout.

The potential curves including the S–O coupling are shown in Fig. 6. The lower four states (group I) dissociate into the $\text{Kr}(^1S_0) + \text{Kr}^+(^2P_{3/2})$ resonance state and the upper two states (group II) into the $\text{Kr}(^1S_0) + \text{Kr}^+(^2P_{1/2})$ state. At the dissociation limits, the calculated IPs of Kr_2 should be comparable with the IPs of the Kr atom. Actually, the IPs generating $\text{Kr}^+(^2P_{3/2})$ and $\text{Kr}^+(^2P_{1/2})$ are 13.999 7 and 14.665 6 eV, respectively [23], compared with our results of Kr_2^+ at $R=12$ bohr, 13.95 and 14.62 eV, respectively. They differ only to within 0.05 eV. The vertical and adiabatic IPs of Kr_2 and the spectroscopic constants of Kr_2^+ are summarized in Table 7 together with the experimental values. Both vertical and adiabatic IPs agree well with experiment to within 0.07 and 0.04 eV, respectively. The calculated dissociation energies are a little smaller than the experimental values.

CONCLUDING REMARKS

We have calculated the potential curves of the 5s Rydberg excited states and ionized states of Kr_2 by the SAC/SAC–CI method. Our potential curves give reliable spectroscopic properties, especially for the absorption region. For the near infrared absorptions from the excited $A(1_u)$ state, we proposed that the $2_g(^3P_2)$ and $1_g(^3P_1)$ states are the candidates of the upper states. The potential curves of the ionized states of Kr_2 are also shown to be reliable. Our vertical and adiabatic IPs compare well with the peaks in the experimental photoionization spectra.

ACKNOWLEDGEMENTS

This study has been supported by the Grant-in-Aid for Scientific Research from the Ministry of Education, Science and Culture. Calculations were carried out at the Computer Centre of the Institute for Molecular Science, and at the Data Processing Centre of Kyoto University.

REFERENCES

- 1 R.H. Lipson, P.E. LaRocque and B.P. Stoicheff, *J. Chem. Phys.*, 134 (1985) 4470.
- 2 P.E. LaRocque, R.H. Lipson, P.R. Herman and B.P. Stoicheff, *J. Chem. Phys.*, 84 (1986) 6627.
- 3 P.R. Herman, P.E. LaRocque and B.P. Stoicheff, *J. Chem. Phys.*, 89 (1988) 4535.
- 4 Y. Mizukami and H. Nakatsuji, *J. Chem. Phys.*, 92 (1990) 6084.

- 5 T.H. Dunning, Jr. and P.J. Hay, *J. Chem. Phys.*, 69 (1978) 134.
- 6 F.X. Gadea, F. Spiegelmann, M.C. Castex and M. Morlais, *J. Chem. Phys.*, 78 (1983) 7270.
- 7 F. Spiegelmann and F.X. Gadea, *J. Phys. (Paris)*, 45 (1984) 1003.
- 8 S. Arai, T. Oka, M. Kogoma and M. Imamura, *J. Chem. Phys.*, 68 (1978) 4595.
- 9 B.R. Brooks, P. Saxe, W.D. Laidig and M. Dupuis, Program Library Gamess (No. 481), Computer Centre of the Institute for Molecular Science, Okazaki, Japan.
- 10 S. Huzinaga, J. Andzelm, M. Klobukowski, E. Radzio-Andzelm, Y. Sakai and H. Tatewaki, *Gaussian Basis Sets for Molecular Calculations*, Elsevier, New York, 1984.
- 11 H. Nakatsuji and K. Hirao, *J. Chem. Phys.*, 68 (1978) 2053.
- 12 H. Nakatsuji, *Chem. Phys. Lett.*, 59 (1978) 362; 67 (1979) 329, 334.
- 13 H. Nakatsuji, *Theor. Chim. Acta*, 71 (1987) 201.
H. Nakatsuji, M. Komori and O. Kitao, in D. Mukherjee (Ed.), *Lecture Notes in Chemistry*, Vol. 50, Springer, Berlin, 1989, pp. 101-122.
- 14 H. Nakatsuji, Program system for SAC and SAC-CI calculations, Program Library No. 146(Y4/SAC), Data Processing Centre of Kyoto University, 1985; Program Library SAC85 (No.1396), Computer Centre of the Institute for Molecular Science, Okazaki, Japan, 1986.
- 15 H. Nakatsuji, *Chem. Phys.*, 72 (1983) 425.
- 16 R.S. Mulliken, *J. Chem. Phys.*, 52 (1970) 5170.
- 17 J.S. Cohen and B. Schneider, *J. Chem. Phys.*, 61 (1974) 3230.
- 18 F. Grein, S.D. Peyerimhoff and R. Klotz, *Theor. Chim. Acta*, 72 (1987) 403.
- 19 C.E. Moore, *Natl. Bur. Stand. (U.S.) Circ. No. 467*, Vol. I, 1949.
- 20 H.M. Hulburt and J.O. Hirschfelder, *J. Chem. Phys.*, 9 (1941) 61; 35 (1961) 1901.
- 21 K.P. Killeen and J.G. Eden, *J. Chem. Phys.*, 83 (1985) 6209.
- 22 Y. Tanaka, K. Yoshino and D.E. Freeman, *J. Chem. Phys.*, 59 (1973) 5160.
- 23 P.M. Dehmer and J.L. Dehmer, *J. Chem. Phys.*, 69 (1978) 125.
- 24 J.T. Moseley, R.P. Saxson, B.A. Huber, P.C. Cosby, R. Abouaf and M. Tadjeddine, *J. Chem. Phys.*, 67 (1977) 1659.